PHYSICAL REVIEW B **90**, 201111(R) (2014)

Observation of quantum states without a semiclassical equivalence bound by a magnetic field gradient

B. Schüler, M. Cerchez, Hengyi Xu, J. Schluck, and T. Heinzel
Condensed Matter Physics Laboratory, Heinrich-Heine-Universität, 40225 Düsseldorf, Germany

D. Reuter
Department Physik, Universität Paderborn, 33098 Paderborn, Germany

A. D. Wieck
Lehrstuhl für Angewandte Festkörperphysik, Ruhr-Universität Bochum, 44780 Bochum, Germany

(Received 23 May 2014; revised manuscript received 3 November 2014; published 24 November 2014)

Resonant transmission through electronic quantum states that exist at the zero points of a magnetic field gradient inside a ballistic quantum wire is reported. Since the semiclassical motion along such a line of zero magnetic field takes place in the form of unidirectional snake trajectories, these states have no classical equivalence. The existence of such quantum states has been predicted more than a decade ago by theoretical considerations. We further show how their properties depend on the amplitude of the magnetic field profile as well as on the Fermi energy.

DOI: 10.1103/PhysRevB.90.201111 PACS number(s): 73.23.−b, 73.21.Hb, 73.20.−r

Magnetic field gradients are ubiquitous in science and technology as key components in, e.g., the Stern-Gerlach setup [1], tokamaks for plasma confinement [2,3], magnetic resonance imaging [4,5], diamagnetic levitation [6], parahydrogen production [7], or read/write heads of computer hard disks based on the giant magnetoresistance [8,9]. In these applications, the magnetic gradient either acts on the electron or nuclear spin, or it affects the dynamics of charged particles, which can be understood within classical pictures. Orbital quantization effects in inhomogeneous magnetic fields have attracted much less attention but may become relevant in some devices as their downsizing continues. Low-dimensional electron gases in semiconductors are excellent systems for studying such effects [10], since the electron Fermi energy can be comparable to the magnetic confinement energy. Furthermore, the electron gases can be exposed to strong magnetic gradients by ferromagnetic [11] or superconductive [12] electrodes. This way, magnetic superlattices [11–13], open magnetic dots [14,15], magnetic stripes which generate electron transport via snake and cycloid trajectories [16], and magnetic barriers [17–22] have been implemented. The measured conductance resonances could all be explained in terms of semiclassical trajectories, while suggestions of quantum states in magnetic field gradients without a classical equivalence [23,24] have remained unobserved.

Here, we report the observation of the quantum states predicted by Reijniers *et al.* [23] to exist at the zero point of a magnetic field step with a sign change in a ballistic quantum wire (QWR). After introducing the experimental setup and the sample characterization, the results are presented and interpreted with the help of numerical simulations.

A GaAs/$Al_xGa_{1-x}As$ heterostructure with a two-dimensional electron gas (2DEG) 45 nm below the surface is used. The shallow design is required for scanning probe lithography but also limits the electron mobility in the dark to 34 $m^2\,V^{-1}\,s^{-1}$ at liquid helium temperatures, while the electron density is $3.8 \times 10^{15}\ m^{-2}$. The sample layout is depicted in Figs. 1(a)–1(c). A Hall bar is patterned by optical lithography. The QWR is defined by scanning probe lithography where local oxidation of the surface leads to depletion of the 2DEG underneath [25]. The lithographic length L and width W of the QWR are 500 and 400 nm, respectively. The 2DEG at the sides of the QWR can be used as in-plane gates [26]. The structure is covered by a homogeneous Cr/Au layer of 10 nm thickness, and a dysprosium (Dy) stripe of width $\ell = 300$ nm and height $h \approx 250$ nm, oriented perpendicular to the wire, is defined on top by electron beam lithography. An external magnetic field $\vec{B}^e = (B^e,0,0)$ magnetizes the Dy stripe along the x direction. The z component $B_z(x)$ of the fringe field forms the desired magnetic field gradient in the transport direction, with a zero point at $x = 0$. This setup represents an experimental implementation of the magnetic step considered in Ref. [23], albeit with a finite slope. This layout has been optimized to provide a strong yet approximately constant magnetic field gradient in the QWR. Variations of the dimensions of this layout are possible only within small parameter intervals. Decreasing ℓ, for example, decreases the amplitude of $B_z(x)$, while increasing ℓ decreases the magnetic gradient and drives the QWR length out of ballisticity. For a magnetic dipole fringe field, $B_z(x)$ in the plane of the 2DEG is given by [20]

$$B_z(x) = \frac{\mu_0 M}{4\pi} \ln\left(\frac{A^-}{A^+}\right), \quad A^{\pm} = \frac{(x \pm \ell/2)^2 + d^2}{(x \pm \ell/2)^2 + (d+h)^2}, \tag{1}$$

where $\mu_0 M$ denotes the magnetization of the Dy stripe and d is the distance between the 2DEG and the bottom of the Dy film. In Fig. 1(c), $B_z(x)$ is plotted for our sample parameters. By Hall magnetometry [17], we estimate the maximum stripe magnetization to $\mu_0 M \approx 2.1$ T [27], corresponding to a maximum value of $|B_z(\pm\ell/2)| = 466$ mT with an approximately constant gradient of $dB_z(x)/dx \approx 3 \times 10^6$ T/m in between. Within a qualitative picture, $B_z(x)$ predominantly influences

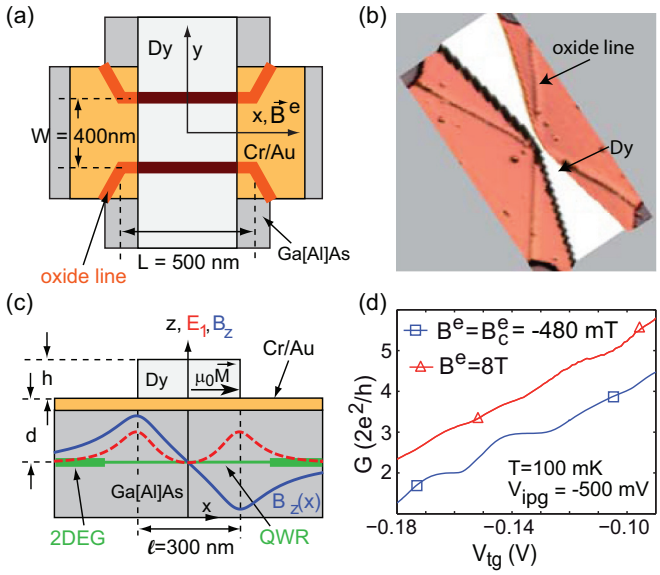

FIG. 1. (Color online) (a) Scheme of the lateral sample layout. (b) Atomic force microscope picture of the Dy stripe on top of the oxide lines. (c) Cross section of the device at $y = 0$, with the magnetic field profile $B_z(x)$ (solid blue line) and the energy of the lowest QWR mode $E_1(x)$ (dashed red line). (d) Conductance of the QWR as a function of the top gate for two applied magnetic fields B^e.

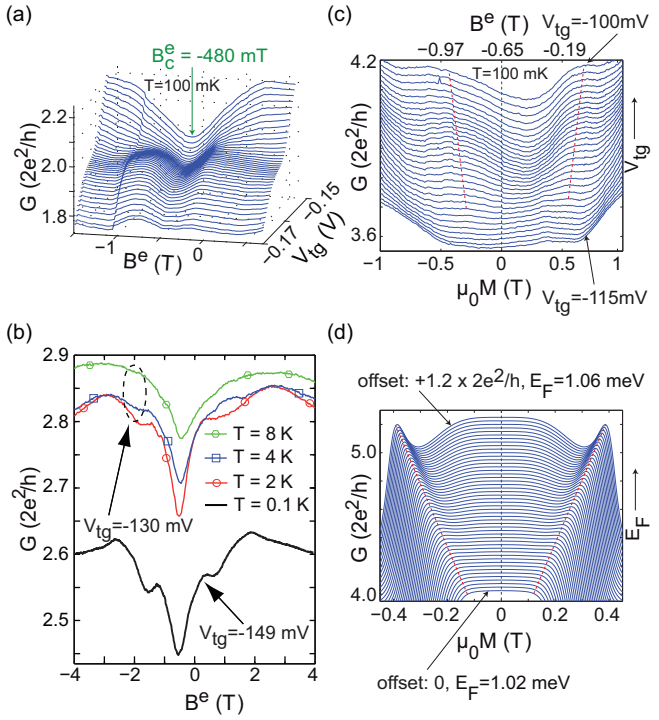

FIG. 2. (Color online) Plots of $G(B^e, V_{tg})$ around the plateaus (a) 2 and (c) 4. In these measurements, B^e was changed in steps of 8 mT and the top gate voltage was varied. In (c), the $\mu_0 M$ axis is also shown, which can be determined from the B^e axis, as described in the text. The red dashed line indicates the evolution of the resonance. (b) Temperature dependence of $G(B^e)$ at fixed gate voltages, as measured in a ^{4}He cryostat with a variable temperature insert. (d) Simulation of the conductance $G(E_F, \mu_0 M)$ as a function of the Dy magnetization and the Fermi energy, in the transition region between conductance plateaus 3 and 4. The peak position is indicated by a red dashed line. Adjacent curves have an offset of $0.024 \times 2e^2/h$ for better visibility.

QWR mode energies via a local diamagnetic shift, as sketched by the red dashed line in Fig. 1(c). Two such magnetic barriers in a series of opposite polarity in a QWR have been discussed theoretically [28–31], in particular, as a tunable spin filter [32–36], but have so far not been implemented experimentally, while experimental studies of magnetic double barriers in 2DEGs [37,38] as well as of single magnetic barriers on QWRs [22,39] have been reported. We have observed the features reported below in two samples and focus on the data from one of them.

Measurements at temperatures $T \geqslant 2$ K were performed in a ^{4}He gas flow cryostat using standard lock-in techniques, while for $T < 1$ K, a ^{3}He/^{4}He dilution refrigerator was used. Both systems are equipped with a superconductive magnet and a rotating sample stage. Parallel alignment of the QWR to $\vec{B}^e$ is established by adjusting the Hall resistance at large B^e to zero.

In Fig. 1(d), the conductance of the QWR as a function of the top gate voltage V_{tg} at the coercive magnetic field $B^e_c = -480$ mT of the Dy stripe is shown. An in-plane gate voltage of $V_{ipg} = -500$ mV was applied in all experiments described below. The electron temperature is $T \approx 100$ mK. Well-developed conductance plateaus with quantized values of $j \times 2e^2/h$ are observed for $j = 2$ and 3 [40,41]. The plateau for $j = 1$ (not shown) is weakly pronounced, most likely due to the greatly decreased electron mobility at low densities in the 2DEG reservoirs, and the visibility of the $j = 4$ plateau is low. By $B^e = 8$ T, the conductance is shifted towards larger values. Since a magnetic depopulation of the wire modes would cause a diamagnetic response, we attribute this shift to the magnetic barrier fields B_z at $x = \pm L/2$, which suppress backscattering in the QWR-2DEG transition regions [42]. This appears plausible considering that our reference QWR without a Dy stripe on top shows, in the regime of six occupied modes at $B^e = 0$, a positive magnetoconductance of about $2e^2/h$ as the homogeneous perpendicular magnetic field is increased from 0 to 0.2 T [27]. In addition, the plateaus tend to get suppressed, and the weak modulation of the conductance traces cannot be assigned to the number of occupied modes, in contrast to homogeneous magnetic fields, which are known to increase the markedness of the conductance plateaus [43]. Spin splitting is excluded as the possible origin, since measurements on the nominally identical QWR without a Dy stripe on top did not show signatures of spin splitting up to $B^e = 10$ T [27]. The effective g factor in the QWRs is thus small. The suppression of the conductance quantization and the emergence of additional features is therefore attributed to the magnetic field profile $B_z(x)$.

Figure 2(a) shows the magnetoconductance $G(B^e, V_{tg})$ of the QWR in the gate voltage interval where two modes are occupied. As a general trend, the conductance increases as $|B^e - B^e_c|$ is increased. Measurements on longer but otherwise comparable QWRs exposed to homogeneous magnetic fields show weak localization in a magnetic field interval $|B_z| \leqslant 20$ mT and a much broader, nearly temperature-independent conductance dip of ≈400 mT width [39], caused by the

magnetic-field-dependent coupling between the quantum wire and the 2DEG mentioned above [42]. We therefore attribute this conductance background to the QWR-2DEG coupling effect, which is of no further interest here. In the following, we focus on the superimposed conductance resonances, visible at distances to B_c^e which increase as V_{tg} is increased. In a cooldown of the same sample in the ^{4}He gas flow cryostat, the same structures are observed, which disappear at a temperature of $T \approx 8$ K [see Fig. 2(b)]. The conductance as a function of the top gate voltage at B_c^e is not shown for the measurement in the ^{4}He gas flow cryostat; it looks similar to Fig. 1(d) but the absolute values on the V_{tg} axis are slightly shifted. The strong temperature dependence of the resonances is in agreement with our interpretation that they have a quantum mechanical origin. Also, these resonant features are absent in the conductance of a 500 nm wide ferromagnetic stripe across a 2DEG, where a smooth, negative magnetoconductance is observed [27]. This suggests that both the magnetic gradient and the electrostatic confinement are required to generate these resonances.

The features are less pronounced around plateaus 3–7, as exemplified for the fourth plateau in Fig. 2(c). The B^e axis (shown on top) can be rescaled to the magnetization $\mu_0 M$ (shown at the bottom) with the help of the hysteresis loop of a Dy film of the same thickness as the Dy stripe [27]. The magnetization behavior of the stripe is not identical to the one of the Dy film due to shape anisotropy, which explains why the measured traces are slightly displaced versus zero magnetization, but plotting the data this way facilitates their comparison to the simulations discussed below. It can be seen that the resonance for $\mu_0 M > 0$ T shifts from $\mu_0 M \approx 650$ mT at $V_{tg} = -100$ mV to ≈500 mT at $V_{tg} = -112$ mV, i.e., over approximately the width of one conductance plateau [see Fig. 1(d)]. Furthermore, these features are observed as a function of both the top gate and the in-plane gate voltages [27].

This phenomenology suggests that the conductance resonances originate from discrete states inside the QWR that form in the presence of $B_z(x)$. Within the model developed by Reijniers *et al.* [23], a magnetic step of the shape $B_z(x) = B_0[\Theta(x) - \frac{1}{2}]$, where $\Theta(x)$ denotes the Heaviside step function and B_0 is the step height, generates a diamagnetic shift everywhere in the quantum wire except at $x = 0$. The effective confinement has the character of a δ potential and only one bound state per mode in the x direction exists. In our experimental implementation, the magnetic step at $x = 0$ has a finite slope and the diamagnetic shift is only present in the interval $|x| \lesssim \ell$, which modifies the states somewhat but does not change their character. Furthermore, the finite extension of the diamagnetic shift is necessary in order to make the bound states accessible for resonant tunneling experiments. Based on this qualitative picture, we interpret the measured resonances with the help of numerical simulations, by using a combination of the tight-binding model with recursive Green's functions [24,31]. The parameters used in the simulation are adapted to our sample, with the exception that $L = 3$ μm, and that due to numerical limitations, the quantum wire (electronic width $W = 300$ nm) is directly attached to reservoirs, such that the transition from the QWR to the 2DEG is not included and the broad positive magnetoconductance background will not be captured. Since the oxide lines written by scanning probe lithography are known to generate

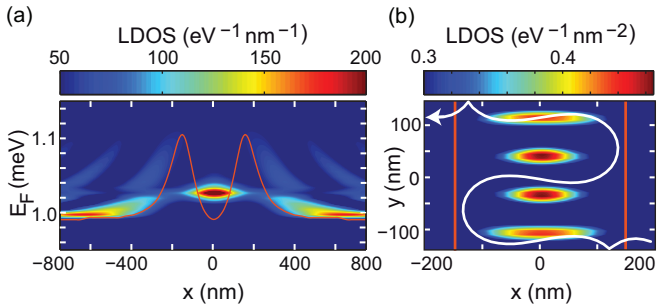

FIG. 3. (Color online) Simulations for a realistic QWR exposed to a magnetic field gradient. (a) The LDOS along the QWR as a function of E_F, calculated for $\mu_0 M = 0.38$ T. One zero-dimensional state is visible at $x = 0$. The red line is the energy of the fourth QWR mode. (b) LDOS(x, y) for the parameters of (c) at $E_F = 1.04$ meV, and a classical electron trajectory (white line). The red lines mark the extremal points of $B_z(x)$.

superparabolic confinement [44], hard walls are assumed. The wire is exposed to the profile $B_z(x)$ given by Eq. (1) with a barrier spacing of $\ell = 300$ nm and an amplitude parametrized by the magnetization $\mu_0 M$. All calculations have been carried out for zero temperature.

We first focus on a clear-cut situation, as found at relatively large Fermi energies E_F where four modes are occupied for $\mu_0 M = 0$, corresponding to Fig. 2(c). In Fig. 2(d), the calculated conductance as a function of $\mu_0 M$ and E_F is shown and can be compared to the data in Fig. 2(c) for magnetic fields larger than B_c^e. In the simulations, the QWR modes get depopulated locally as either E_F is decreased or $\mu_0 M$ is increased. A single resonance per wire mode which shifts diamagnetically is seen. The measured resonant features are thus in reasonable agreement with the simulations, considering that the possible effects of B_x are neglected and the magnetization characteristics of the Dy stripe as well as the shape of the quantum wire confinement potential are not exactly known.

The origin of the resonances becomes apparent with the help of the local density of states (LDOS). In Fig. 3(a), the LDOS as a function of x and the Fermi energy, integrated along the y direction, is shown for $\mu_0 M = 0.38$ T, which is a plausible magnetization in view of the data shown in Fig. 2(c) [27]. A zero-dimensional state at $x = 0$ emerges. Its LDOS at $E_F = 1.04$ meV as a function of x and y is shown in Fig. 3(c). It corresponds to a standing wave in the transverse direction, and the number of nodes shows that it originates from the fourth wire mode.

As pointed out above, one bound state per wire mode is present if the magnetic step is infinitely sharp. In our implementation, however, the magnetic field gradient is finite, such that several quantized states per wire mode along the x direction become possible. Also, a striking paramagnetic shift of the bound states is found in Ref. [23], which reflects their increasing localization at the magnetic step as B_0 is increased. This is in contrast to our implementation, where the effective potential becomes narrower as the magnetization increases, which causes the energies of the states to increase with increasing magnetization.

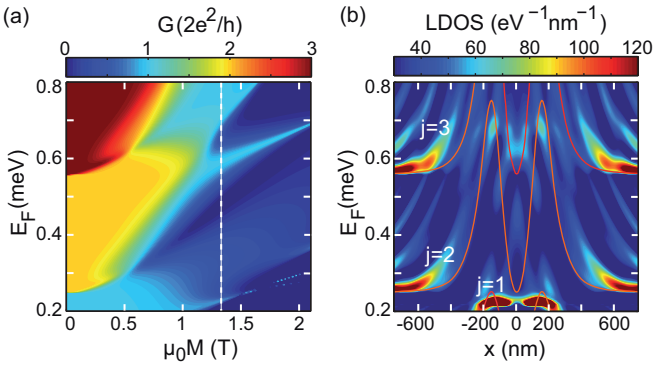

FIG. 4. (Color online) Numerical studies of the system over a wide range of magnetizations and low Fermi energies. The calculated conductance is shown in (a). The dashed line marks the magnetization of $\mu_0 M = 1.33$ T used for the LDOS as a function of E_F and the x coordinate shown in (b). Here, j denotes the mode index.

The consequences of the deviations of our experimental implementation to the ideal magnetic step in a QWR are illustrated in Fig. 4, where the conductance over a wide range of Fermi energies and magnetizations is shown. As $\mu_0 M$ increases, the weakly pronounced conductance modulations evolve into sharp resonances, reflecting the increased effective confinement [see Fig. 4(a)]. Furthermore, a second resonance per QWR mode can be formed. This can be seen, for example, in the conductance as a function of $\mu_0 M$ for $E_F \approx 0.62$ meV, or as a function of E_F at $\mu_0 M = 1.33$ T. For the latter case, we show the LDOS (E_F, x) in Fig. 4(b). Here, two LDOS maxima at $E_F \approx 0.62$ meV and $\approx$0.68 meV are visible, both belonging to the third QWR mode. Note that the bound state with larger energy shows a node in the x direction at $x = 0$. This energy structure reflects the fact that in our sample, magnetic confinement in the x direction is weaker than the electrostatic one in the y direction.

To summarize, we have observed resonant transmission through a ballistic quantum wire via magnetically bound states that reside at the zero point of a magnetic field gradient, as suggested by Reijniers *et al.* [23]. These quantum states have no classical equivalence. We observe up to two such states per wire mode, all with a diamagnetic response. Both of these findings are in contrast to the original proposal, and we have explained these deviations by the finite steepness of the magnetic step in our experimental implementation. The presence of several bound states per mode is furthermore of relevance regarding an experimental realization of the suggested magnetic barrier spin filters [33–36], since their energy spacing may be comparable to the spin splitting energy and thereby influence on the spin polarization.

The authors would like to thank HHU Düsseldorf for financial support and I. V. Zozoulenko for valuable discussions in relation to the Green's function formalism. A.D.W. is grateful to Mercur Pr-2013-0001, BMBF - Q.com-H 16KIS0109, and to the DFH/UFA for support in the CDFA-05-06.

[1] W. Gerlach and O. Stern, Z. Phys. **9**, 349 (1922).
[2] I. E. Tamm, in *Plasma Physics and the Problem of Controlled Thermonuclear Reactions* (AN SSSR, Moscow, 1958), Vol. 1, p. 3.
[3] A. D. Sakharov, in *Plasma Physics and the Problem of Controlled Thermonuclear Reactions* (Ref. [2]), p. 20.
[4] P. C. Lauterbur, Nature (London) **242**, 190 (1973).
[5] A. N. Garroway, P. K. Grannell, and P. Mansfield, J. Phys. C **7**, L457 (1974).
[6] M. V. Berry and A. K. Geim, Eur. J. Phys. **18**, 307 (1997).
[7] A. M. Juarez, D. Cubric, and G. C. King, Meas. Sci. Technol. **13**, N52 (2002).
[8] M. N. Baibich, J. M. Broto, A. Fert, F. Nguyen Van Dau, F. Petroff, P. Etienne, G. Creuzet, A. Friederich, and J. Chazelas, Phys. Rev. Lett. **61**, 2472 (1988).
[9] G. Binasch, P. Grünberg, F. Saurenbach, and W. Zinn, Phys. Rev. B **39**, 4828 (1989).
[10] A. Nogaret, J. Phys.: Condens. Matter **22**, 253201 (2010).
[11] P. D. Ye, D. Weiss, R. R. Gerhardts, M. Seeger, K. von Klitzing, K. Eberl, and H. Nickel, Phys. Rev. Lett. **74**, 3013 (1995).
[12] H. A. Carmona, A. K. Geim, A. Nogaret, P. C. Main, T. J. Foster, M. Henini, S. P. Beaumont, and M. G. Blamire, Phys. Rev. Lett. **74**, 3009 (1995).
[13] S. Izawa, S. Katsumoto, A. Endo, and Y. Iye, J. Phys. Soc. Jpn. **64**, 706 (1995).
[14] K. S. Novoselov, A. K. Geim, S. V. Dubonos, Y. G. Cornelissens, F. M. Peeters, and J. C. Maan, Phys. Rev. B **65**, 233312 (2002).
[15] D. Uzur, A. Nogaret, H. E. Beere, D. A. Ritchie, C. H. Marrows, and B. J. Hickey, Phys. Rev. B **69**, 241301 (2004).
[16] A. Nogaret, S. J. Bending, and M. Henini, Phys. Rev. Lett. **84**, 2231 (2000).
[17] F. G. Monzon, M. Johnson, and M. L. Roukes, Appl. Phys. Lett. **71**, 3087 (1997).
[18] M. Johnson, B. R. Bennett, M. J. Yang, M. M. Miller, and B. V. Shanabrook, Appl. Phys. Lett. **71**, 974 (1997).
[19] V. Kubrak, A. Neumann, B. L. Gallagher, P. C. Main, M. Henini, C. H. Marrows, and B. J. Hickey, J. Appl. Phys. **87**, 5986 (2000).
[20] T. Vančura, T. Ihn, S. Broderick, K. Ensslin, W. Wegscheider, and M. Bichler, Phys. Rev. B **62**, 5074 (2000).
[21] M. Cerchez, S. Hugger, T. Heinzel, and N. Schulz, Phys. Rev. B **75**, 035341 (2007).
[22] A. Tarasov, S. Hugger, H. Xu, M. Cerchez, T. Heinzel, I. V. Zozoulenko, U. Gasser-Szerer, D. Reuter, and A. D. Wieck, Phys. Rev. Lett. **104**, 186801 (2010).
[23] J. Reijniers, A. Matulis, K. Chang, F. M. Peeters, and P. Vasilopoulos, Europhys. Lett. **59**, 749 (2002).
[24] H. Xu, T. Heinzel, M. Evaldsson, S. Ihnatsenka, and I. V. Zozoulenko, Phys. Rev. B **75**, 205301 (2007).
[25] R. Held, S. Lüscher, T. Heinzel, K. Ensslin, and W. Wegscheider, Appl. Phys. Lett. **75**, 1134 (1999).

[26] A. D. Wieck and K. Ploog, Appl. Phys. Lett. **56**, 928 (1990).
[27] See Supplemental Material at http://link.aps.org/supplemental/10.1103/PhysRevB.90.201111 for the resonances that appear in quantum wire modes two to six and that provide measurements that exclude alternative explanations of the origin of these resonances.
[28] M. Governale and D. Boese, Appl. Phys. Lett. **77**, 3215 (2000).
[29] F. Zhai, Y. Guo, and B.-L. Gu, Phys. Rev. B **66**, 125305 (2002).
[30] G. Papp and F. M. Peeters, J. Appl. Phys. **107**, 063718 (2010).
[31] H. Xu, T. Heinzel, and I. V. Zozoulenko, Phys. Rev. B **84**, 035319 (2011).
[32] H. Z. Xu and Y. Okada, Appl. Phys. Lett. **79**, 3119 (2001).
[33] M.-W. Lu, L.-D. Zhang, and X.-H. Yan, Phys. Rev. B **66**, 224412 (2002).
[34] K. C. Seo, G. Ihm, K.-H. Ahn, and S. J. Lee, J. Appl. Phys. **95**, 7252 (2004).
[35] M. B. A. Jalil, J. Appl. Phys. **97**, 024507 (2005).
[36] F. Zhai and H. Q. Xu, Appl. Phys. Lett. **88**, 032502 (2006).
[37] V. Kubrak, F. Rahman, B. L. Gallagher, P. C. Main, M. Henini, C. H. Marrows, and M. A. Howson, Appl. Phys. Lett. **74**, 2507 (1999).
[38] J. U. Bae, T. Y. Lin, Y. Yoon, S. J. Kim, J. P. Bird, A. Imre, W. Porod, and J. L. Reno, Appl. Phys. Lett. **91**, 022105 (2007).
[39] S. Hugger, H. Xu, A. Tarasov, M. Cerchez, T. Heinzel, I. V. Zozoulenko, D. Reuter, and A. D. Wieck, Phys. Rev. B **78**, 165307 (2008).
[40] B. J. van Wees, H. van Houten, C. W. J. Beenakker, J. G. Williamson, L. P. Kouwenhoven, D. van der Marel, and C. T. Foxon, Phys. Rev. Lett. **60**, 848 (1988).
[41] D. A. Wharam, T. J. Thornton, R. Newbury, M. Pepper, H. Ahmed, J. E. F. Frost, D. G. Hasko, D. C. Peacock, D. A. Ritchie, and G. A. C. Jones, J. Phys. C **21**, L209 (1988).
[42] H. van Houten, C. W. J. Beenakker, P. H. M. van Loosdrecht, T. J. Thornton, H. Ahmed, M. Pepper, C. T. Foxon, and J. J. Harris, Phys. Rev. B **37**, 8534 (1988).
[43] B. J. van Wees, L. P. Kouwenhoven, H. van Houten, C. W. J. Beenakker, J. E. Mooij, C. T. Foxon, and J. J. Harris, Phys. Rev. B **38**, 3625 (1988).
[44] A. Fuhrer, S. Lüscher, T. Heinzel, K. Ensslin, W. Wegscheider, and M. Bichler, Phys. Rev. B **63**, 125309 (2001).